Current Microbiology (2023) 80:251
https://doi.org/10.1007/s00284-023-03357-2

Antifungal Activity of Nanobiocomposite Films Based on Silver Nanoparticles Obtained Through Green Synthesis

Eduardo José Juca Mallmann[1] · Francisco Afrânio Cunha[1,2] · Enzo Victorino Hernandez Agressott[3] · Fernando Lima de Menezes[1] · Rita de Cássia Carvalho Barbosa[2] · Roxeane Teles Martins[4] · Maria da Conceição dos Santos Oliveira Cunha[5,6] · Maria Veraci Oliveira Queiroz[5] · Henrique Douglas Melo Coutinho[7] · John Eversong Lucena de Vasconcelos[8] · Pierre Basílio Almeida Fechine[1]

Received: 20 November 2022 / Accepted: 29 May 2023

Abstract
The high incidence of *Candida albicans* infections has raised concerns regarding side effects and drug resistance, compounded by a limited number of alternative drugs. Silver nanoparticles (AgNPs) have prominent antimicrobial activity, but effective administration remains a challenge. In this study, AgNPs were synthesized via a green chemistry approach, using glucose as a reducing agent, and incorporated into an agar matrix to form a film (AgFilm). The AgNPs and AgFilm were characterized by Ultraviolet–visible (UV–vis) spectroscopy, Fourier transform infrared (FTIR) spectroscopy, dynamic light scattering (DLS), powder X-ray diffraction (PXRD), scanning electron microscopy (SEM), and atomic force microscopic (AFM). The UV–Vis spectra of the AgNPs and AgFilm showed bands at 415 and 413 nm, respectively. The PXRD and UV–Vis data suggest that the growth of AgNPs was effectively inhibited in the AgFilm. The diameter of AgNPs dispersed in AgFilm was 76 ± 42 nm, and the thickness of the film and 35 ± 3 µm. The antifungal activity of AgFilm was evaluated against 20 strains of *C. albicans*, demonstrating high antifungal activity with an inhibition zone of 19 ± 2 mm. Therefore, AgFilm could be a promising option for the treatment of superficial *C. albicans* infections.

Introduction

In recent years, fungal infections have emerged as a major problem in human health. Around 13 million infections and more than 1.5 million deaths per year are caused by fungi worldwide, affecting mainly immunocompromised people, such as those HIV-positive, transplant patients, and those undergoing cancer therapy [1, 2]. Despite these facts, fungal infections are still neglected by many public health authorities while drug resistance, as occurs in bacterial infections, becomes more and more common [3].

Candida spp. is the most frequent cause of human fungal infections. *C. albicans* is the most common and most pathogenic, being responsible for about 50% of cases,

✉ Henrique Douglas Melo Coutinho
hdmcoutinho@gmail.com

✉ Pierre Basílio Almeida Fechine
fechine@ufc.br

[1] Grupo de Química de Materiais Avançados (GQMat) – Departamento de Química Analítica e Físico-Química, Universidade Federal do Ceará (UFC), Campus do Pici, CP 12100, Fortaleza, CE 60451-970, Brazil

[2] Departamento de Análises Clínicas e Toxicológicas da Universidade Federal do Ceará-UFC , Rua Capitão Francisco Pedro 1210, Rodolfo Teófilo, Fortaleza, CE 60270-430, Brazil

[3] Departamento de Física, Universidade Federal do Ceará (UFC), Campus do Pici, Caixa Postal 6030, Fortaleza, CE 60440-970, Brazil

[4] Laboratório de Análises Clínicas e Toxicológicas da Universidade Federal do Ceará, Fortaleza, Brazil

[5] Universidade Estadual do Ceará. Programa de Pós-Graduação Cuidados Clínicos em Enfermagem e Saúde, Fortaleza, Ceará, Brazil

[6] Professora da Faculdade Princesa do Oeste, Crateus, Ceará, Brazil

[7] Laboratorio de Microbiologia e Biologia Molecular, Departamento de Biologia Química, Universidade Regional do Cariri-URCA, Crato, Brazil

[8] CECAPE College, Juazeiro do Norte, Av. Padre Cícero, 3917, São José, CE 63024-015, Brazil

Published online: 23 June 2023

followed by C. *glabrata*, C. *parapsilosis*, C. *krusei,* and C. *tropicalis* [3]. These species have the striking ability to form a biofilm, an assemblage of cells in extracellular polymeric substances strongly adhered to surfaces, which provides a protective barrier against human resistance mechanisms [4, 5]. Thus, control by common antifungals becomes challenging, which leads to the pursuit of new drugs.

Drugs available for candidiasis include polyenes (amphotericin B), triazoles (fluconazole, itraconazole, voriconazole) and echinocandins (caspofungin, micafungin, anidulafungin) [2]. However, issues such as neurotoxicity and drug resistance have led to the use of novel materials, such as metallic nanoparticles [4]. Among these, silver nanoparticles (AgNPs) are prominent because of their high microbial toxicity by inducing intracellular production of reactive oxygen species (ROS), combined with their biocompatibility and easy availability [3]. They have numerous applications: in dressings, intravenous and urinary catheters, sutures, orthodontic adhesives, surgical masks, and films for use in the manufacturing, pharmaceutical, and food industries [6, 7].

AgNPs can be synthesized by a wide range of protocols, either by reduction with hazardous chemicals such as sodium borohydride, or by cleaner approaches through green chemistry using renewable and low-cost materials, such as using reducing sugars, plant extracts, and microorganisms [4]. Since AgNPs are very prone to agglomerate, which weakens their microbial activity, they require surface modification or attachment to support [2]. Accordingly, they have been combined with various polymers, especially biopolymers such as agar, gelatin, alginate, pullulan, starch, chitosan, and cellulose [8, 9]. These biopolymers have easy film-forming capabilities and many of them are biocompatible, allowing them to be applied to skin lesions as a breathable physical barrier to the entry of microorganisms [10]. In this sense, the incorporation of AgNPs in these films is promising for a controlled release system to treat already existing infections [5].

Among the several biopolymers that can incorporate AgNPs, one of the most widely used is agar [11, 12], a complex polysaccharide found in red algae (agarophytes) cell walls [13]. Films containing AgNPs dispersed in agar matrix arouse great interest due to their antimicrobial and mechanical properties [14, 15].

Two main approaches are used to incorporate AgNPs into films: the *in-situ* method, when the synthesis of the nanoparticles takes place in the matrix that will form the composite; and the *ex-situ* method, when AgNPs are previously synthesized, purified, characterized, and only afterward incorporated into a matrix to form a nanobiocomposite [16]. The *ex-situ* procedure was applied in this work since it allows greater control of the synthesis and yields material with fewer impurities.

The nanobiocomposite introduced in this work features as a novelty the process used in its production and its application to prevent the growth of fungal strains.

This study aimed to produce and characterize AgNPs through a green methodology and incorporate them into an agar film to obtain a nanobiocomposite with antifungal activity against C. albicans.

Materials and Methods

Materials

All of the reagents, including silver nitrate (Dinâmica—São Paulo—Brazil, purity > 99%), sorbitol (Sigma USA—purity > 98%), agarose (Bio Basic—Canada—purity > 98%), sodium dodecyl sulfate (SDS) (Vetec—Brazil—purity > 98%), NaOH (Dinâmica—Brazil—purity > 98%) were commercial products of analytical grade and used as purchased without further purification.

Most of the *Candida albicans* strains used in this work were obtained from the Yeast Collection of the Yeast Microbiology Laboratory at the Department of Clinical and Toxicological Analysis of the Faculty of Pharmacy, Dentistry and Nursing of the Federal University of Ceará (LML/DACT/FFOE/UFC). These strains, totaling 20, were obtained from samples collected from patients between 2015 and 2020 and were rigorously purified and identified by biochemical, phenotypic, and molecular tests, previously reported [17, 18]. In addition, the standard strain ATCC 10 231 was also used. Previously, they were stored in a viable state at − 80 °C.

AgNPs and AgFilm Fabrication

The AgNPs were synthesized using glucose as a reducing agent and SDS as a stabilizer, based on a previously published method that used ribose to reduce silver ions [18]. This process is illustrated in Fig. 1. Firstly, 500.0 mL of a solution containing 1.1×10^{-2} mol•L^{-1} glucose, 5×10^{-3} mol•L^{-1} $AgNO_3$, and 3.5×10^{-2} mol•L^{-1} SDS were prepared. Then, 1.0 mL of NaOH 0.2 mol/L was added to accelerate the reaction, and the mixture was kept at 50 °C for 1 h under constant stirring. The reaction was considered complete when the solution acquired a yellow color characteristic of the colloidal suspension with AgNPs. Subsequently, the AgNPs were purified by centrifugation at 10,000 rpm for 20 min and then redispersed in distilled water for further use. To prepare the Agfilm, 1.5 g of agarose and 0.5 g of sorbitol were solubilized in 100.0 mL of the AgNPs suspension at 80 °C under constant stirring for 1 h. After this step, the solution was poured into polystyrene Petri dishes. The plates were placed in an oven at 60 °C to complete the drying process. AgFilms were removed from

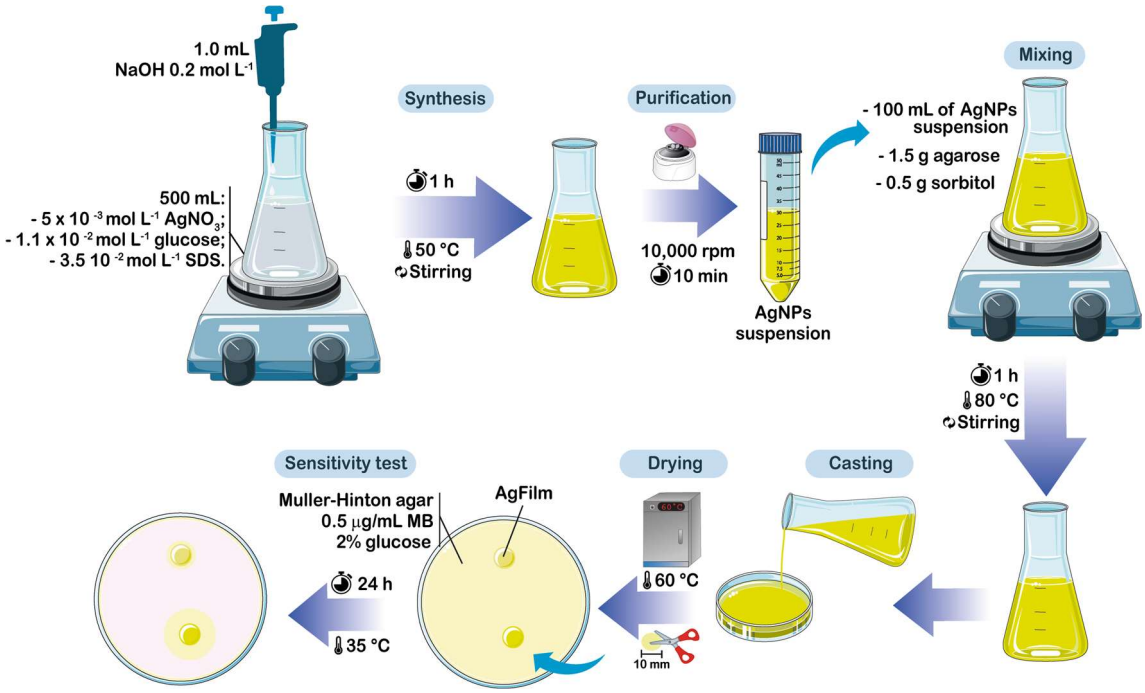

Fig. 1 Schematic drawing of the procedures for the synthesis of AgNPs and their application in anti-*Candida* composite films

the plates and then characterization and antifungal activity tests were performed [11].

Characterization of AgNPs and AgFilm

Ultraviolet–Visible (UV–vis) Spectroscopy

To confirm the production of AgNPs, the obtained solution and the AgFilm were subjected to UV–vis spectroscopy in the 300–700 nm range in a Thermo Scientific GENESYS ™ 10 s spectrophotometer.

Size

The average size of the AgNPs was measured in the colloidal solutions using dynamic light scattering (DLS), a non-invasive backscatter technology to determine the Brownian motion of particles in solution. By analyzing fluctuations in the scattered light intensity, DLS provides valuable information about the size distribution of the particles in a colloidal solution. The measurements were performed using a Zetasizer Nano ZS, Malvern Instruments-UK.

Fourier Transform Infrared (FTIR) Spectroscopy

FTIR spectroscopy measurements were performed to confirm the functionalization of the AgNPs by SDS and their incorporation into the films, using the AgNPs and AgFilm samples. The measurements were carried out using a Perkin-Elmer FTIR Spectrum ONE spectrophotometer, with spectral data recorded at a resolution of 4 cm^{-1} and a range of 4000–750 cm^{-1}. To prepare the samples for analysis, they were dried in a vacuum desiccator, ground into a fine powder, mixed with KBr, and compressed into pellets.

Powder X-Ray Diffraction (PXRD)

The AgNPs and AgFilm samples were ground into a fine powder and placed on a 2.5 cm × 2.5 cm glass support. Diffractogram measurements were then taken in the 2θ range of 30°–80°, using Cu-Ka and nickel radiation, with an X-ray powder diffractometer with Bragg–Brentano geometry set to operate at 40 kV and 30 mA. The samples were analyzed using a PAN analytical X-pert Pro MRD (Amsterdam, Netherlands).

AgFilm Thickness

The film thickness was measured using a digital caliper (Dial Thickness gage 7301, Mitutoyo, Tokyo, Japan) with an accuracy of 0.01 mm. The measurements were taken in 20 different regions of the AgFilm, and the results were calculated as average and standard deviation.

Microscopic Features

Scanning electron microscopy (SEM) was carried out in a Quanta-450 (FEI) electron microscope with a field-emission

gun (FEG), a 100 mm stage and an X-ray detector (model 150, Oxford) for energy-dispersive X-ray spectroscopy (EDS). The EDS analysis was performed to confirm the presence of silver and other elements in the samples. The Atomic Force Microscopy (AFM) procedures were performed using a Multimode Nanoscope IIIa (Bruker, CA, USA), in Tapping Mode (or intermittent mode). In this scanning mode, the AFM tip touches the sample surface with beats of similar amplitude to the resonance amplitude of the AFM cantilever. A rectangular probe model TESPA7 (Veeco) with a nominal spring constant of k = 20–80 N/m and resonance frequency of 291–326 kHz was used. The scan parameters for the nanoparticles imaging were 0.5 Hz scan rate and 512 × 512 lines resolution. The images were analyzed to determine the size and distribution of the AgNPs, as well as the surface morphological features of the AgFilm. The diameters of the particles were measured using the ImageJ software.

Antifungal Activity of AgFilm

The antifungal activity of the AgFilm was evaluated by comparing the growth inhibition zones caused by the AgFilm to those of the control disks free of AgNPs. It was used 20 strains of *Candida albicans* isolated from patients treated in public hospitals in the city of Fortaleza, Ceará, Brazil. To evaluate the antifungal activity of the AgFilm, the diffusion method was used on a Muller-Hinton agar solid medium that was supplemented with 2% glucose and 0.5 µg/mL methylene blue, as shown in Fig. 1. AgFilm disks were cut to 10 mm in diameter and placed on previously prepared culture media by seeding *C. albicans* solutions. The plates were then incubated at 35 °C for 24 h. After this time, the plates were photographed, and the inhibition zones of fungal growth caused by the AgFilm disks were measured using ImageJ software. The growth inhibition zone was determined by measuring from the center of the disk to the edge at which no fungal growth occurred [19]. All tests were performed in triplicate. Disks free of AgNPs were used as control.

Statistical Analysis

The results of the demonstrating the reduction of inhibition zone as mean ± standard deviation, evaluated statistically by analysis of variance (one-way ANOVA) using GraphPad Prism software. Differences were considered significant when $P < 0.05$. The assay was performed in triplicate.

Results

Aspect of the Materials

As shown in the insets of Fig. 2A and the figure available in the supplementary material, the AgNPs suspension and the film had a consistent and homogeneous appearance. The suspension was clear and free of any visible sediments and had a light orange color, while the film was flexible with a thickness of 35 ± 3 µm (mean ± SD) and a more intense orange color.

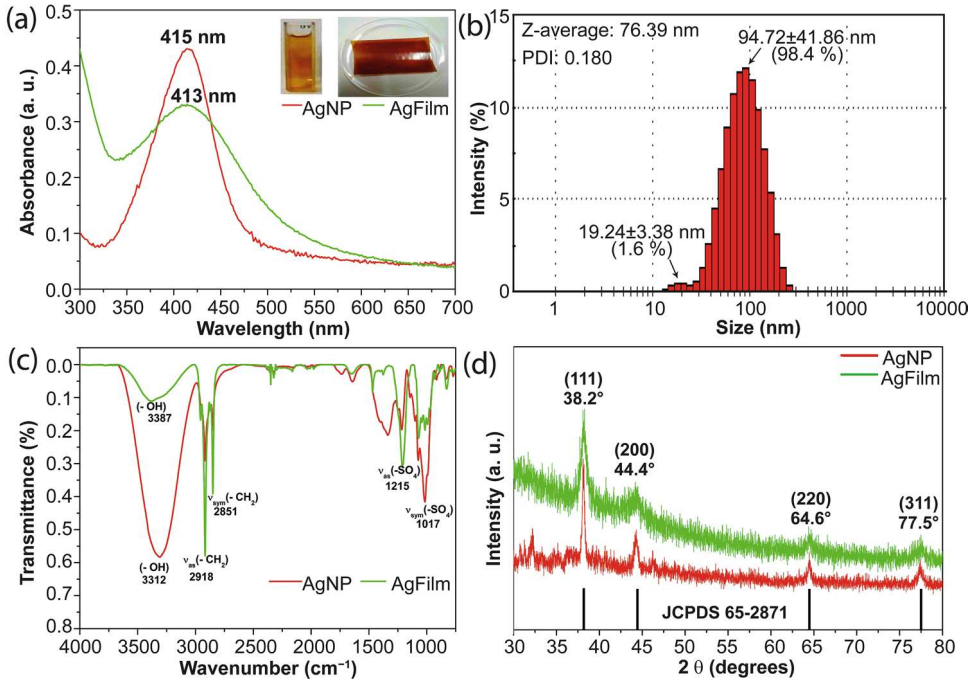

Fig. 2 Characterization of AgNPs and AgFilm samples: **a** UV–Vis absorption spectra of the AgNPs suspension and film (**b**) average hydrodynamic size histogram for AgNPs aqueous suspension, obtained by DLS analyses; **c** FTIR spectra of the dried AgNPs and the film powder macerated on KBr pellets; **d** X-ray diffractogram for the film and the dried AgNPs

Ultraviolet–Visible (UV–vis) Spectroscopy

Figure 2A shows the UV–visible absorption spectra for the colloidal AgNPs suspension and for the AgFilm. The colored suspension (yellow line) and film (red line) spectra indicate the presence of Ag nanoparticles (inset photo in Fig. 2A). Furthermore, the strong absorption bands at around 415 (nm) (AgNPs) and 413 nm (AgFilm) indicate that the nanoparticles have a strong surface plasmon resonance (SPR) in the visible wavelength range. The full width at half maximum (FWHM) for the nanoparticles supported on films (162 nm) was broader compared to that observed for suspension (83 nm).

Colloidal Properties of the AgNPs Suspension

Figure 2B shows the particle size distribution of the AgNPs in suspension analyzed by DLS. The analysis revealed a mean value of 76 ± 42 nm (mean $\pm$ SD), with a low polydispersity index (PDI) of 0.180, indicating the monodispersity of AgNPs in the sample.

FTIR

To confirm the presence of SDS on the surface of AgNPs, which may have contributed to the results obtained by DLS, they were subjected to FTIR analysis. This characterization technique is powerful for elucidating the structure and chemical composition of materials, providing information about the nature of the chemical bonds present. Therefore, it was also used to analyze the AgFilm.

Figure 2C shows the FTIR spectra of AgNPs and AgFilm. The stretching and deformation vibrational modes related to methyl groups are, respectively, observed at 2918 and 2851 cm^{-1} in the AgNPs and AgFilm samples. These bands are attributed to the CH groups from SDS, which was used as a stabilizer in the synthesis of these particles. SDS has a long, saturated, unbranched carbon chain consisting of 14 carbons atoms. The bands are intensified in the film due to the CH groups in the polymer matrix (agar) adding to SDS vibrations, thereby increasing the band signal related to CH groups [20].

The bands observed at 1215 cm^{-1} and 1017 cm^{-1} are assigned to the symmetric and asymmetric stretching of sulfonated groups ($-SO_4$) in SDS, respectively [21]. The bands at 3387 cm^{-1} in AgFilm and 3312 cm^{-1} in AgNPs can be attributed to hydroxyl group stretching vibrations [22]. The higher band intensity in AgNPs can be explained by incomplete drying.

PXRD

As previously discussed, UV–Vis analysis provides information for identifying AgNPs due to their characteristic plasmonic band. Nevertheless, to provide information regarding structural ordering and crystalline phase composition XRD analysis is crucial. Figure 2D shows the diffraction patterns of the AgNPs and AgFilm samples. In both diffractograms, silver diffractions peaks at 2θ angles of 38.2, 44.4, 64.6 and 77.5° were present, which are correlated to the crystal planes (111), (200), (220), and (311), respectively.

These diffraction peaks provide valuable information about the crystal structure of the AgNPs. In this case, the patterns indicate that AgNPs have a face-centered cubic (fcc) structure (JCPDS, No. 65–2871), which is commonly observed in metallic nanoparticles. Furthermore, the peak intensities suggest the samples have a crystalline nature. The agar matrix is a typically amorphous material, composed mainly of the monosaccharide galactose, and broad, diffuse peaks have been reported at around 13 and 20° for this polymer [15, 23, 24]. This amorphous character can be seen by the low-angle background in the AgFilm diffractogram.

It is worth mentioning that the Bragg reflections (200), (220) and (311) are weaker and broader than the reflection in the (111) plane, which indicates crystal growth in the preferential direction (111), commonly observed in polymeric films [22, 25]. Moreover, the broader peaks were observed in the AgFilm sample.

Microstructural Analysis

The morphology of the AgNPs within the polymer matrix was determined using SEM and AFM. These techniques are complementary and valuable for analyzing the surface of a material, as SEM provides a wide and detailed view of the sample while AFM has higher resolution and provides topographic images.

Figure 3A, C and D show that the AgNPs are predominantly spherical in shape and are well distributed throughout the surface of the AgFilm. Figure 3D shows a three-dimensional scanning view of the film (topographic mode), confirming the efficient dispersion of AgNPs within the polymer matrix [26].

Figure 3B shows the EDS spectrum of AgFilm, where the peak at around 3.0 keV indicates the presence of silver, as described in the literature [27]. The EDS confirms the existence of AgNPs within the AgFilm [9]. Composition analysis of the AgFilm showed a range of constituents, including carbon as the main component and a silver content of 39.49%. Considering the silver concentration in the AgNPs suspension around 1500 µg/mL, a silver content (w/w) lower than 7% was expected. Such divergence is due to EDS analyzing only a close area (a small portion) of the sample and only

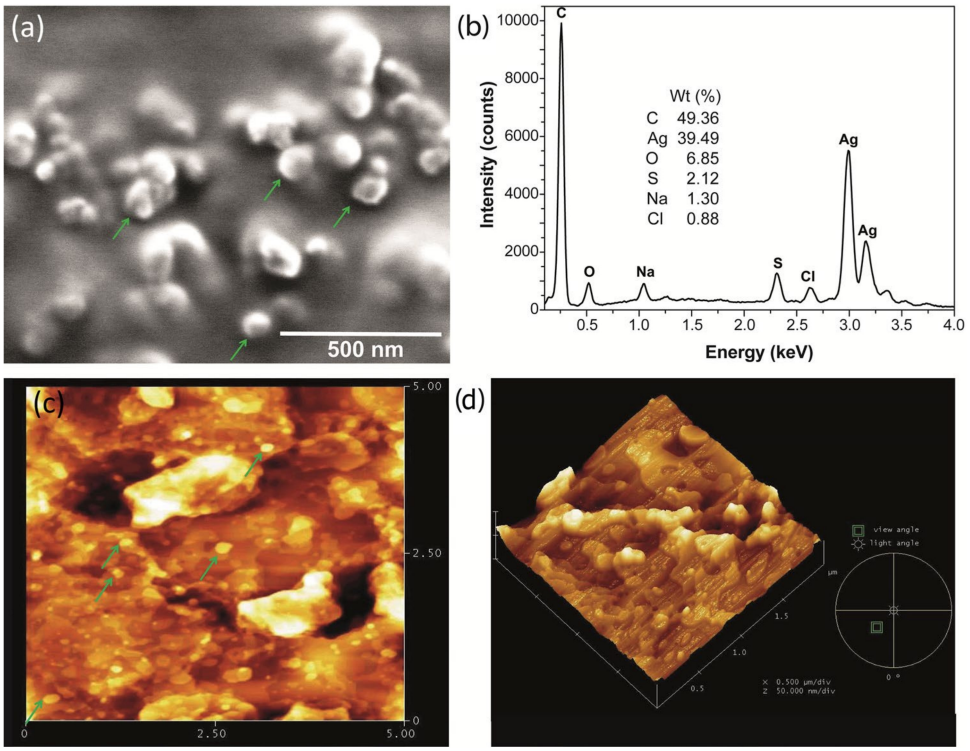

Fig. 3 **a** SEM image of AgFilm; **b** EDX Spectrum of AgFilm. **c** and **d** AFM images of AgFilm. The green arrows indicate AgNPs incorporated in the AgFilm

its surface. Additionally, the EDS technique is susceptible to errors due to either the nature or the preparation of the sample. The other constituents, in smaller amounts, were oxygen, sulfur, and sodium chloride. The occurrence of these minor elements is due to the precursor materials used to synthesize AgNPs and obtain AgFilm. Furthermore, sulfur (S) is derived from SDS and agarose (a sulfated polymer).

From the analysis of 100 particle sizes in SEM and AFM images using ImageJ software, the size distribution histograms of the AgNPs within the AgFilm were obtained. The SEM images revealed particles with an average size of 87 ± 28 nm (Fig. 4A), whereas AFM images showed an average size of 78 ± 31 nm (Fig. 4B). These values are consistent with those obtained using other techniques: DLS, AFM and SEM. It is noteworthy that both SEM and AFM images show some clusters formed during the AgFilm drying process, which could explain the higher standard deviations observed in the histograms of Figs. 4A and B.

Antifungal Activity of AgFilm

The antifungal activity of the AgFilm was evaluated in triplicate by testing 20 strains of *C. albicans*, and the results are shown in Fig. 5. Although the antibacterial and antifungal

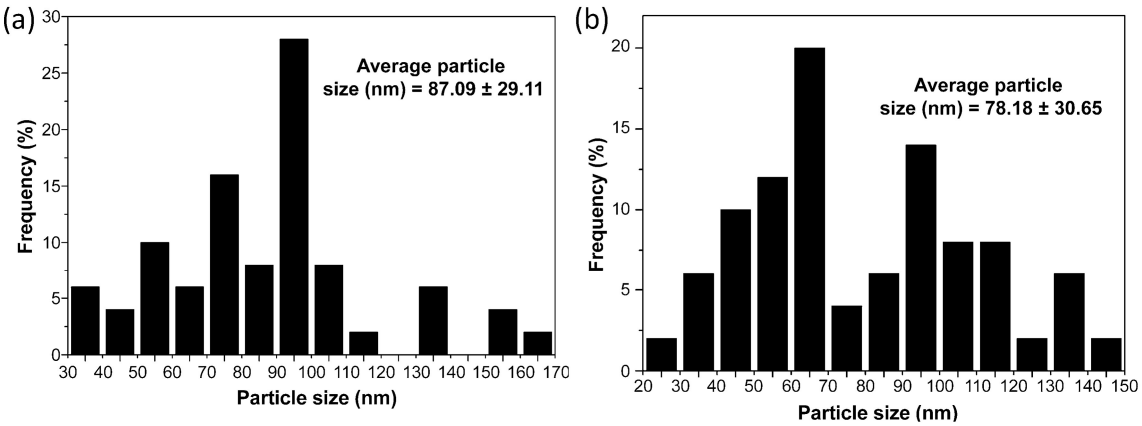

Fig. 4 Size distribution histograms of the AgNPs embedded in AgFilm, obtained by SEM (**a**) and by AFM (**b**)

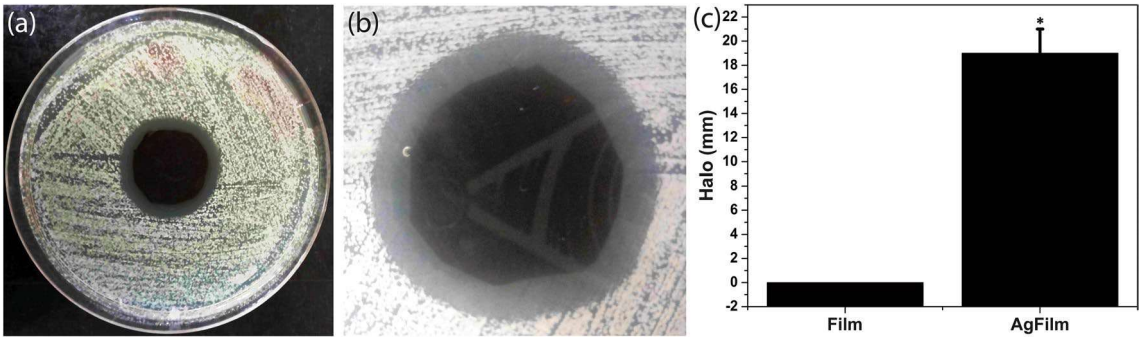

Fig. 5 Petri dish demonstrating the growth inhibition zone of *C. albicans* caused by AgFilm (**a**) and close-up view of the inhibition halo due to its application (**b**). A comparison between the halo formed by disks with and without AgNPs is shown in **c**. "*" $P < 0.05$ and indicates significant differences between groups. Statistical significance was determined by one-way ANOVA.

activities of silver nanoparticles have been already reported in the literature [26], many studies are conducted with only one standard strain [28]. However, due to the high number of *C. albicans* infections worldwide, it is expected this specie undergoes mutations to develop resistance to drugs and immune system. In this study, 20 distinct strains of *C. albicans* obtained from patient samples between 2015 and 2020 were tested. Thus, using samples with varying strains obtained from biological samples allowed for a more thorough evaluation of the product, considering its actual application.

The inhibition zones for the treatments of the 20 *C. albicans* strains with AgFilm had an average inhibition halo of 19 ± 2 mm (Fig. 5C). The agar matrix exhibited no antifungal effect, thereby providing evidence that the growth inhibition was solely attributable to the presence of AgNPs. According to literature, AgNPs exhibit potent antifungal activity against *C. albicans* by inhibiting their budding process, leading to the disruption of the plasma membrane integrity, and cell death [4]. The aforementioned activity is well demonstrated in Figs. 5A and B, where the gray zones encircling the AgFilm disks indicates the absence of fungal growth.

Discussion

Glucose is a cheap and non-toxic reagent, sometimes used as a reduction agent in reactions to synthesize AgNPs [29]. The synthesis conditions of AgNPs can vary and incorporate other substances. In this study, SDS was used as a stabilizer, sodium hydroxide as a catalyst, and sorbitol to provide elasticity to AgFilm [21, 30, 31]. The embedding of AgNPs into the film was performed by an *ex-situ* method, which consists in adding the as-prepared AgNPs to agar. AgNPs bind to the polymer generating a nanostructured film with an important biological property. Agar films described in the literature have a similar thickness to the ones obtained in this work, which enables its technological applications [11, 16]. The incorporation of sorbitol in the film preparation protocol has the purpose of providing plasticity and strength. The agar films described in the literature have no sorbitol addition, which makes them brittle and hard to handle [19].

The findings by UV–Vis spectroscopy for the AgNPs film and suspension were consistent with predictions and earlier experiments for spherical silver nanoparticles with an average particle size below 20 nm [32, 33]. Previous studies have shown that the strong SPR band occurs around 420 nm when AgNPs are dispersed in other polymeric matrices, close to those found in this work [13, 22].

The intensity and the FWHM of the plasmon band could also be correlated to the average particle size of the nanoparticles in suspension [32, 33]. According to Mie's theory, the FWHM becomes broader as the size of the nanoparticles in suspension decreases [34]. Additionally, previous studies have reported redshift and increase in the band intensity as the size of AgNPs increases [33]. Therefore, these findings are indications of growth of the particles that were left in suspension [32, 33]. Due to their presumed good dispersion in the composite, the AgNPs onto the AgFilm were kept further apart and prevented from clustering and growing. It is also important to consider that the polymeric chains present in the agar film may have attenuated signal absorption, leading to an inconsistent interpretation. Therefore, further characterizations were conducted to validate these results.

Further evidence for a lower particle growth in the film was found by XRD, with the broadened peaks for this sample. The smaller the crystallite size D, the broader the peaks, as predicted by Sherrer's equation: $D = K \cdot \lambda / \beta \cdot \cos\theta$, where K is the shape factor, λ is the X-ray wavelength, β is the full width at half maximum, and θ is the diffraction angle (in radians) [35].

Even with the growth of the particles, DLS analysis indicated that the AgNPs in suspension were monodispersed.

This is a desirable property in nanotechnology, since a narrow size distribution implies higher colloidal stability, easier dispersion, and uniformity of material quality and response. However, the size value found by DLS was higher than expected from the UV–Vis spectrum.

It is worth mentioning that the mean particle size in DLS analysis represents the hydrodynamic diameter of the particles, which is calculated considering the Brownian motion of the particles in solution and assuming that they have a spherical isotropic shape. Moreover, the organic layer covering the surface of the AgNPs is considered in this analysis, unlike other methods such as Transmission Electron Microscopy (TEM) and SEM, which measure the actual size of the particle (the metal core) [36].

In addition, the hydrodynamic diameter of AgNPs can vary depending on the preparation method and experimental conditions [36]. For instance, a study of nano-bioconjugates showed by DLS analysis a single population of AgNPs in the size range of 20–40 nm [37]. In another recent study, AgNPs were synthesized by chemical (using $NaBH_4$) and green synthesis (using Sargassum species extract), and hydrodynamic diameters of 12.7 ± 0.7 and 27 ± 3 nm were obtained, respectively [36].

The AgNPs stabilization indicated by DLS is due to the presence of negatively charged sulfate groups on the nanoparticles' surface, resulting from SDS, a surfactant widely employed to prepare stable and monodisperse nanoparticles [38, 39]. This was confirmed by FTIR analysis. In AgFilm, the intermolecular interaction of these groups with the hydroxyls of the agar polysaccharide chain (indicated by FTIR) favors their stabilization indicated by UV–Vis. Furthermore, the shift and divergence in the relative intensities of the bands for the film and those for the AgNPs indicates that chemical bonds occurred between the agar matrix polymer and the AgNPs [11, 40].

Despite the stabilizing interaction provided by SDS, clusters were observed in the SEM and AFM images, which seem to be formed in the drying process itself. The clustering of AgNPs in the film occur dues to a solvent change, and an imbalance of aggregation forces between the AgNPs and polymeric fibers. Van der Waals forces, electrostatic and magnetic forces no longer act exclusively between the AgNPs, but also between them and the polymer structure [31]. However, UV–Vis and DRX analysis revealed higher stability of the AgNPs within the agar matrix. Well-dispersed and aggregation-protected AgNPs are desired in the application as an antifungal, as they allow for controlled and prolonged delivery of AgNPs through the polymer matrix [41].

Products containing AgNPs have shown efficacy against a broad range of microorganisms, making them promising tools for infection control [15]. AgNPs synthesized using saffron tepal extract, at a concentration of 2650 $mg \cdot L^{-1}$, exhibited an inhibition zone of 16 mm against *C. albicans* [42]. Conversely, AgNPs synthesized through $NaBH_4$ mediated reduction showed maximum inhibition zone of only 6.5 mm at a dosage of 100 $mg\ L^{-1}$ [43]. Malathi et al. conducted experiments with *C. albicans*, specifically the 10,261 and 5314 strains, and inhibition zones of 22 and 20 mm were observed, respectively, after using AgNPs synthesized with *Hyptis suaveolens* leaf extract [44]. Ediyilyam et al. synthesized AgNPs using the leaf extract of *Mussaenda frondosa* and obtained an inhibition zone to *C. albicans* of 16 mm with a 1000 µg/L AgNPs suspension [45].

Few studies have evaluated the inhibition zones of composite films containing AgNPs. Compared to AgNPs suspensions, AgNP films have a lower diffusion rate since the nanoparticles are entrapped in the matrix for prolonged and controlled delivery. The AgFilm developed in this study demonstrated outstanding results against *C. albicans* strains, with an average inhibition zone of 19 ± 2 mm, indicating its potential as an effective antifungal agent. The Agfilm figures as a promising alternative to traditional antimicrobial agents for treating infections caused by *C. albicans*.

C. albicans is an opportunistic fungus responsible for various types of skin lesions, and an agar film containing active AgNPs can be used in bandages to prevent and aid in the treatment of these infections, particularly in burned patients and diabetics who are highly susceptible to bacterial and fungal infections [46]. This procedure could possibly reduce the side effects of common drugs. The films developed in this work showed high antifungal activity and could be of great use in the food and pharmaceutical industries.

Conclusions

The nanobiocomposite (AgFilm) manufactured in this study showed physical features comparable to those found in other films reported in the literature. The AgNPs were preserved within their structure, showing suitable thickness and transparency. Moreover, as evidenced by UV–Vis and XRD analyses, the agar matrix inhibited the growth of the AgNPs, thereby increasing their stability and retaining their antifungal properties. The preliminary antifungal activity assays suggest that AgFilm could be a valuable tool in treating skin infections caused by *C. albicans*.

Supplementary Information The online version contains supplementary material available at https://doi.org/10.1007/s00284-023-03357-2.

Acknowledgements The authors want to gratefully acknowledge the collaborators at the Central Analítica of the Universidade Federal do Ceará, the Laboratório de Microscopia- Física- UFC, the Laboratório

de Raios-X- UFC, the Laboratório de Materiais Avançados- UFC e the Laboratório de Microbiologia de Leveduras-UFC.

Funding This research was supported by the funding agencies Conselho Nacional de Desenvolvimento Científico e Tecnológico (CNPq) and Fundação Cearense de Pesquisa (Funcap).

Data Availability The data presented in this study are available on request from the corresponding author. The strains are preserved in the Yeast Collection of the Laboratory of Yeast Microbiology of the Department of Clinical and Toxicological Analysis of the School of Pharmacy, Dentistry and Nursing of the Federal University of Ceará (LML/DACT/FFOE/UFC).

Code Availability Not applicable.

Declarations

Conflict of interest The authors declare that there is no conflict of interest that could have appeared to influence the research work reported in this paper.

Ethical Approval The samples used in this work are from a collection and we are a faithful depositary in Brazil, which makes an ethics committee unnecessary.

Consent to Participations All samples used were received by a faithful depositary, de-identified, without any personal information from the patients.

Consent for Publications All patients' personal information was de-identified, thus keeping their personal information confidential, even before the samples were deposited in our collection.

References

1. Rayens E, Norris KA (2022) Prevalence and healthcare burden of fungal infections in the United States, 2018. Open Forum Infect Dis. https://doi.org/10.1093/OFID/OFAB593
2. Zhou L, Zhao X, Li M et al (2021) Antifungal activity of silver nanoparticles synthesized by iturin against *Candida albicans* in vitro and in vivo. Appl Microbiol Biotechnol 105:3759–3770. https://doi.org/10.1007/S00253-021-11296-W/FIGURES/8
3. Jia D, Sun W (2021) Silver nanoparticles offer a synergistic effect with fluconazole against fluconazole-resistant Candida albicans by abrogating drug efflux pumps and increasing endogenous ROS. Infect Genet Evol 93:104937. https://doi.org/10.1016/J.MEEGID.2021.104937
4. Nadhe SB, Singh R, Wadhwani SA, Chopade BA (2019) *Acinetobacter* sp. mediated synthesis of AgNPs, its optimization, characterization and synergistic antifungal activity against *C. albicans*. J Appl Microbiol 127:445–458. https://doi.org/10.1111/JAM.14305
5. Soumbo M, Scarangella A, Villeneuve-Faure C et al (2020) Combined effect of proteins and AgNPs on the adhesion of yeast *Candida albicans* on solid silica surfaces. Proc IEEE Conf Nanotechnol. https://doi.org/10.1109/NANO47656.2020.9183494
6. Rhim JW, Park HM, Ha CS (2013) Bio-nanocomposites for food packaging applications. Prog Polym Sci 38:1629–1652. https://doi.org/10.1016/J.PROGPOLYMSCI.2013.05.008
7. Seo SY, Lee GH, Lee SG et al (2012) Alginate-based composite sponge containing silver nanoparticles synthesized in situ. Carbohydr Polym 90:109–115. https://doi.org/10.1016/J.CARBPOL.2012.05.002
8. Cheviron P, Gouanvé F, Espuche E (2014) Green synthesis of colloid silver nanoparticles and resulting biodegradable starch/silver nanocomposites. Carbohydr Polym 108:291–298. https://doi.org/10.1016/J.CARBPOL.2014.02.059
9. Hassabo AG, Nada AA, Ibrahim HM, Abou-Zeid NY (2015) Impregnation of silver nanoparticles into polysaccharide substrates and their properties. Carbohydr Polym 122:343–350. https://doi.org/10.1016/J.CARBPOL.2014.03.009
10. de Paula GA, Costa NN, da Silva TM et al (2022) Polymeric film containing pomegranate peel extract as a promising tool for the treatment of candidiasis. Nat Prod Res. https://doi.org/10.1080/14786419.2022.2064464/SUPPL_FILE/GNPL_A_2064464_SM9878.PDF
11. Ghosh S, Kaushik R, Nagalakshmi K et al (2010) Antimicrobial activity of highly stable silver nanoparticles embedded in agar–agar matrix as a thin film. Carbohydr Res 345:2220–2227. https://doi.org/10.1016/J.CARRES.2010.08.001
12. Muthuswamy E, Ramadevi SS, Vasan HN et al (2007) Highly stable Ag nanoparticles in agar-agar matrix as inorganic-organic hybrid. J Nanoparticle Res 9:561–567. https://doi.org/10.1007/S11051-006-9071-Z/METRICS
13. Silva TH, Alves A, Ferreira BM, et al (2013) Materials of marine origin: a review on polymers and ceramics of biomedical interest. 57:276–307. https://doi.org/10.1179/1743280412Y.0000000002
14. Rhim JW, Wang LF, Hong SI (2013) Preparation and characterization of agar/silver nanoparticles composite films with antimicrobial activity. Food Hydrocoll 33:327–335. https://doi.org/10.1016/J.FOODHYD.2013.04.002
15. Shukla MK, Singh RP, Reddy CRK, Jha B (2012) Synthesis and characterization of agar-based silver nanoparticles and nanocomposite film with antibacterial applications. Bioresour Technol 107:295–300. https://doi.org/10.1016/J.BIORTECH.2011.11.092
16. Rhim JW, Wang LF, Lee Y, Hong SI (2014) Preparation and characterization of bio-nanocomposite films of agar and silver nanoparticles: Laser ablation method. Carbohydr Polym 103:456–465. https://doi.org/10.1016/J.CARBPOL.2013.12.075
17. Cunha FA, da Cunha MCSO, da Frota SM et al (2018) Biogenic synthesis of multifunctional silver nanoparticles from *Rhodotorula glutinis* and *Rhodotorula mucilaginosa*: antifungal, catalytic and cytotoxicity activities. World J Microbiol Biotechnol 34:1–15. https://doi.org/10.1007/s11274-018-2514-8
18. Mallmann EJJ, Cunha FA, Castro BNMF et al (2015) Antifungal activity of silver nanoparticles obtained by green synthesis. Rev Inst Med Trop Sao Paulo 57:165–167. https://doi.org/10.1590/s0036-46652015000200011
19. Kanmani P, Rhim JW (2014) Antimicrobial and physical-mechanical properties of agar-based films incorporated with grapefruit seed extract. Carbohydr Polym 102:708–716. https://doi.org/10.1016/J.CARBPOL.2013.10.099
20. Viana RB, Da Silva ABF, Pimentel AS (2012) Infrared spectroscopy of anionic, cationic, and zwitterionic surfactants. Adv Phys Chem. https://doi.org/10.1155/2012/903272
21. Azócar I, Vargas E, Duran N et al (2012) Preparation and antibacterial properties of hybrid-zirconia films with silver nanoparticles. Mater Chem Phys 137:396–403. https://doi.org/10.1016/J.MATCHEMPHYS.2012.09.042
22. Zhao X, Xia Y, Li Q et al (2014) Microwave-assisted synthesis of silver nanoparticles using sodium alginate and their antibacterial activity. Colloids Surf A 444:180–188. https://doi.org/10.1016/J.COLSURFA.2013.12.008
23. Kumar S, Jahan K, Verma A et al (2022) Agar-based composite films as effective biodegradable sound absorbers. ACS Sustain Chem Eng 10:8242–8253. https://doi.org/10.1021/ACSSU

SCHEMENG.2C00168/ASSET/IMAGES/LARGE/SC2C00168_0008.JPEG
24. Audeh DJSA, Alcázar JB, Barbosa CV et al (2014) Influence of the NiO nanoparticles on the ionic conductivity of the agar-based electrolyte. Polimeros 24:8–12. https://doi.org/10.4322/POLIMEROS.2014.055/PDF/POLIMEROS-24-ESPECIAL-8.PDF
25. Pandey S, Goswami GK, Nanda KK (2012) Green synthesis of biopolymer–silver nanoparticle nanocomposite: an optical sensor for ammonia detection. Int J Biol Macromol 51:583–589. https://doi.org/10.1016/J.IJBIOMAC.2012.06.033
26. Pinto RJB, Fernandes SCM, Freire CSR et al (2012) Antibacterial activity of optically transparent nanocomposite films based on chitosan or its derivatives and silver nanoparticles. Carbohydr Res 348:77–83. https://doi.org/10.1016/J.CARRES.2011.11.009
27. Kim SC, Kim JW, Yoon GJ et al (2013) Antifungal effects of 3D scaffold type gelatin/Ag nanoparticles biocomposite prepared by solution plasma processing. Curr Appl Phys 13:S48–S53. https://doi.org/10.1016/J.CAP.2013.01.035
28. Pinto RJB, Almeida A, Fernandes SCM et al (2013) Antifungal activity of transparent nanocomposite thin films of pullulan and silver against *Aspergillus niger*. Colloids Surf B 103:143–148. https://doi.org/10.1016/J.COLSURFB.2012.09.045
29. Kahrilas GA, Haggren W, Read RL et al (2014) Investigation of antibacterial activity by silver nanoparticles prepared by microwave-assisted green syntheses with soluble starch, dextrose, and arabinose. ACS Sustain Chem Eng 2:590–598. https://doi.org/10.1021/SC400487X/SUPPL_FILE/SC400487X_SI_001.PDF
30. Pettegrew C, Dong Z, Muhi MZ et al (2014) Silver nanoparticle synthesis using monosaccharides and their growth inhibitory activity against gram-negative and positive bacteria. ISRN Nanotechnol 2014:1–8. https://doi.org/10.1155/2014/480284
31. Tan Z, Abe H, Naito M, Ohara S (2010) Oriented growth behavior of Ag nanoparticles using SDS as a shape director. J Colloid Interface Sci 348:289–292. https://doi.org/10.1016/J.JCIS.2010.04.018
32. Slistan-Grijalva A, Herrera-Urbina R, Rivas-Silva JF et al (2005) Assessment of growth of silver nanoparticles synthesized from an ethylene glycol–silver nitrate–polyvinylpyrrolidone solution. Physica E 25:438–448. https://doi.org/10.1016/J.PHYSE.2004.07.010
33. Slistan-Grijalva A, Herrera-Urbina R, Rivas-Silva JF et al (2005) Classical theoretical characterization of the surface plasmon absorption band for silver spherical nanoparticles suspended in water and ethylene glycol. Physica E 27:104–112. https://doi.org/10.1016/J.PHYSE.2004.10.014
34. Jain S, Mehata MS (2017) Medicinal plant leaf extract and pure flavonoid mediated green synthesis of silver nanoparticles and their enhanced antibacterial property. Sci Rep 71(7):1–13. https://doi.org/10.1038/s41598-017-15724-8
35. Thirumagal N, Jeyakumari AP (2020) Structural, optical and antibacterial properties of green synthesized silver nanoparticles (AgNPs) using Justicia *adhatoda* L. leaf extract. J Clust Sci 31:487–497. https://doi.org/10.1007/S10876-019-01663-Z/TABLES/2
36. López-Miranda JL, Esparza R, González-Reyna MA et al (2021) Sargassum influx on the mexican coast: a source for synthesizing silver nanoparticles with catalytic and antibacterial properties. Appl Sci 11:4638. https://doi.org/10.3390/APP11104638
37. Goswami AM, Sarkar TS, Ghosh S (2013) An ecofriendly synthesis of silver nano-bioconjugates by penicillium citrinum (MTCC9999) and its antimicrobial effect. AMB Express 3:1–9. https://doi.org/10.1186/2191-0855-3-16/FIGURES/5
38. Gao Y, Ma Q (2022) Bacterial infection microenvironment-responsive porous microspheres by microfluidics for promoting anti-infective therapy. Smart Med. https://doi.org/10.1002/SMMD.20220012
39. Abraham L, Thomas T, Pichumani M (2022) Vivid structural colors of photonic crystals: self-assembly of monodisperse silica nano-colloids synthesized using an anionic surfactant. Chem Phys 563:111682. https://doi.org/10.1016/J.CHEMPHYS.2022.111682
40. Kanmani P, Rhim JW (2014) Properties and characterization of bionanocomposite films prepared with various biopolymers and ZnO nanoparticles. Carbohydr Polym 106:190–199. https://doi.org/10.1016/J.CARBPOL.2014.02.007
41. Tran PA, Hocking DM, O'Connor AJ (2015) In situ formation of antimicrobial silver nanoparticles and the impregnation of hydrophobic polycaprolactone matrix for antimicrobial medical device applications. Mater Sci Eng C 47:63–69. https://doi.org/10.1016/J.MSEC.2014.11.016
42. Khorasani S, Ghandehari Yazdi AP, Saadatfar A et al (2022) Valorization of saffron tepals for the green synthesis of silver nanoparticles and evaluation of their efficiency against foodborne pathogens. Waste Biomass Valorization 13:4417–4430. https://doi.org/10.1007/S12649-022-01791-0/FIGURES/10
43. Khatoon UT, Velidandi A, Nageswara Rao GVS (2023) Sodium borohydride mediated synthesis of nano-sized silver particles: their characterization, anti-microbial and cytotoxicity studies. Mater Chem Phys. https://doi.org/10.1016/J.MATCHEMPHYS.2022.126997
44. Malathi S, Manikandan D, Nishanthi R et al (2022) Silver nanoparticles, synthesized using *Hyptis suaveolens* (L.) Poit and their antifungal activity against *Candida* spp. ChemistrySelect 7:e202203050. https://doi.org/10.1002/SLCT.202203050
45. Ediyilyam S, George B, Shankar SS et al (2021) Chitosan/gelatin/silver nanoparticles composites films for biodegradable food packaging applications. Polymers (Basel) 13:1680. https://doi.org/10.3390/POLYM13111680/S1
46. Peršin Z, Maver U, Pivec T et al (2014) Novel cellulose based materials for safe and efficient wound treatment. Carbohydr Polym 100:55–64. https://doi.org/10.1016/J.CARBPOL.2013.03.082